Assessing Hydrologic Response to Climate Change of a Stream Watershed Using SLURP Hydrological Model

5 authors, including:

So-Ra Ahn
Texas A&M AgriLife Research Center at El Paso
47 PUBLICATIONS   **202** CITATIONS

Seongjoon Kim
Konkuk University
224 PUBLICATIONS   **1,984** CITATIONS

Assessing Hydrologic Response to Climate Change of a Stream Watershed Using SLURP Hydrological Model

So Ra Ahn*, Geun Ae Park**, In Kyun Jung***, Kyoung Jae Lim****, and Seong Joon Kim*****

....

Abstract

The impact on streamflow and groundwater recharge considering future potential climate and land use changes was assessed using Semi-distributed Land-Use Runoff Process (SLURP) continuous hydrologic model. The model was calibrated and verified using 4 years (1999-2002) daily observed streamflow data for a 260.4 km² watershed which has been continuously urbanized during the past couple of decades. The model was calibrated and validated with 0.72 average coefficient of determination and 0.69 average Nash-Sutcliffe model efficiency respectively. For the future climate change assessment, three GCMs (MIROC3.2hires, ECHAM5-OM, and HadCM3) of IPCC A2, A1B, and B1 scenarios from 1977 to 2099 were adopted, and the data was corrected using 30 years (1977-2006, baseline period) ground weather data and downscaled by Change Factor simple statistical method. The future land uses were predicted by Cellular Automata-Markov technique using the time series land use data of Landsat images. The 2080 land uses showed that the forest and paddy areas decreased 10.8% and 6.2% respectively while the urban area increased 14.2%. For the future vegetation canopy prediction, a linear regression between monthly Normalized Difference Vegetation Index (NDVI) from NOAA/AVHRR images and monthly mean temperature using eight years (1997-2004) data was derived for each land use class. The 2080s highest NDVI value was 0.64 while the current highest NDVI value was 0.51. The future assessment showed that the annual streamflow increased up to 52.8% for 2080 HadCM3 A2 scenario and decreased up to 14.5% for 2020 ECHAM5-OM A1B scenario respectively. The seasonal results showed that the spring streamflow of three GCMs clearly increased while the summer streamflow decreased for MIROC3.2 hires and ECHAM5-OM, and increased for HadCM3 corresponding to each precipitation change of GCMs. The portion of future predicted Evapotranspiration (ET) about precipitation increased up to 3.0% in MIROC3.2 hires, 16.0% in ECHAM5-OM, and 20.0% in HadCM3 respectively. The future soil moisture content slightly increased compared to 2002 soil moisture. The increase of soil moisture resulted in the increase of groundwater recharge except ECHAM5-OM. The increase of summer ET gives us a decision making in advance for the security of future water demands. Thus the increased streamflow during spring period has to be managed more carefully and efficiently than the present situation.

Keywords: *SLURP, land use change, climate change, GCM, downscaling, NDVI, hydrologic components*

....

1. Introduction

The Intergovernmental Panel on Climate Change (IPCC) report reaffirms that the climate is changing in ways that cannot be explained by natural variability and that "global warming" is occurring (IPCC, 2001). This global warming due to the build-up of greenhouse gases is likely to have significant impacts on the hydrologic cycle (Arnell, 1999; IPCC, 2001). The hydrologic cycle will be intensified, with more evaporation and more precipitation, but the extra precipitation will be unequally distributed around the globe (Zhang *et al.*, 2007a). Precipitation patterns and amounts may change in complex ways, varying both in time and space (Loaiciga *et al.*, 1996; Arnell, 1999). These changes have important implications for river flows, runoff and regional water resource management (Forch *et al.*, 1996; Westmacott and Burn, 1997).

An assessment of the hydrological impacts of climate change is essential to plan for future water resources management (Aleix *et al.*, 2007). Modeling hydrologic impacts of climate change involves simulation results from General Circulation Models (GCMs), which are the most credible tools designed to simulate time series of climate variables globally (Ghosh and Mujumdar,

*Graduate Student, Dept. of Civil and Environmental System Engineering, Konkuk University, Seoul 143-701, Korea (E-mail: ahnsora@konkuk.ac.kr)

**Member, Post-doctoral Researcher, Dept. of Civil and Environmental System Engineering, Konkuk University, Seoul 143-701, Korea (E-mail: dolpin2000@konkuk.ac.kr)

***Member, Post-doctoral Researcher, Dept. of Civil and Environmental System Engineering, Konkuk University, Seoul 143-701, Korea (E-mail: nemoik@konkuk.ac.kr)

****Associate Professor, Dept. of Regional Infrastructures Engineering, Kangwon National University, Chuncheon 200-701, Korea (E-mail: kjlim@kangwon.ac.kr)

*****Member, Professor, Dept. of Civil and Environmental System Engineering, Konkuk University, Seoul 143-701, Korea (Corresponding Author, E-mail: kimsj@konkuk.ac.kr)

2008). Recently, a number of climate impacts on runoff have been accomplished by coupling GCM outputs and hydrological model. Kite *et al.* (1994) estimated runoffs by connection of Canadian Climate Center (CCC) GCM and SLURP model for Mackenzie and Columbia basins of Canada. Gellens and Rouline (1998) used seven GCMs and IRMB (Integrated Runoff Model) to analyze the impact of climate change for runoffs of eight basins of Belgium. Ahn *et al.* (2001) used water balance model to investigate runoff change of Daecheong-dam watershed of South Korea by using the results of GCM. Andersson *et al.* (2006) used four GCMs and Pitman hydrological model to assess the impact of various development and climate change scenarios on downstream river flow in Okavango river basin. Merritt *et al.* (2006) evaluated the hydrologic response to scenarios of climate change in Okanagan basin of British with the connection of three GCMs and UBC watershed model. Zhang *et al.* (2007b) estimated the effect of potential climate change on available streamflow volume in Luohe river basin using two GCMs and SWAT model.

A number of investigations of hydrologic response have focused on changes in streamflow volumes or timing due to climate change, and the streamflow to climate change reports that is closely related to the change in precipitation. The hydrologic cycle is going to be affected by climate change together with land use and vegetation canopy changes. Land use change directly affects Evapotranspiration (ET), infiltration and soil water storage changing the dynamics of surface runoff, subsurface runoff and groundwater recharge. The vegetation canopy change by future temperature increase certainly influences the evaporation from soils and transpiration from the vegetation. Therefore, we need to consider the future potential change of land use and vegetation canopy for fair water resources evaluation by future climate change.

The main objective of this study is to assess the potential impact of climate change on streamflow and groundwater recharge of a stream watershed considering future changes of land use and vegetation canopy condition. The future land use information was prepared by applying the modified Cellular Automata (CA)-Markov technique (Lee and Kim, 2007) using the past temporal series of Landsat land cover data. The future vegetation canopy condition of each land use was predicted by the NOAA Normalized Difference Vegetation Index (NDVI) versus air temperature relationship. The SLURP model (Kite, 1975) was applied to evaluate the future climate impact on streamflow, soil moisture and groundwater recharge using the three GCMs (MIROC3.2 hires, ECHAM5-OM, HadCM3) data by three Special Report on Emissions Scenarios (SRES) A1B, A2 and B1.

2. SLURP Model Description

The basin-level hydrological model, SLURP was adopted for assessing future climate and land use impact on streamflow and the state variables; ET, soil moisture content and groundwater recharge. SLURP is a continuous semi-distributed hydrological model to simulate the behavior of a watershed at many points, and is particularly useful for studies in which land cover is expected to change and climate change studies (Kite, 1993). The model was originally designed to use land cover information from satellite imagery.

After dividing the watershed into Aggregated Simulation Areas (ASAs), the model routes precipitation through the appropriate processes and generates outputs (evaporation, transpiration and runoff) and changes in storage (canopy interception, snowpack and soil moisture). Runoffs are accumulated from each land cover within an ASA using a time-contributing area relationship for each land cover and the combined runoff is converted to streamflow and routed between each ASA.

Each element of the ASA land cover is represented by four nonlinear reservoirs representing canopy interception, snowpack, fast storage, and slow storage (Fig. 1). The outputs of each vertical water balance include evaporation, transpiration, runoff, groundwater flow, and changes in canopy storage, snowpack, soil moisture and groundwater (Kite, 2000).

3. Model Setup

3.1 Study Area Description
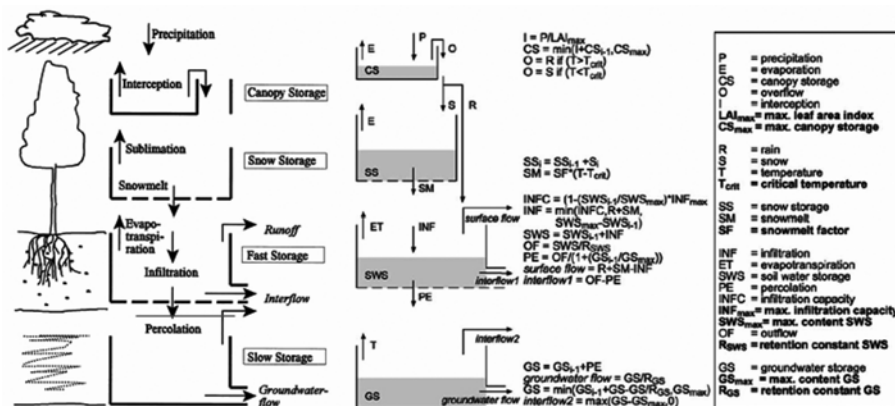The study area (260.4 km²) which has Gyeongan water level

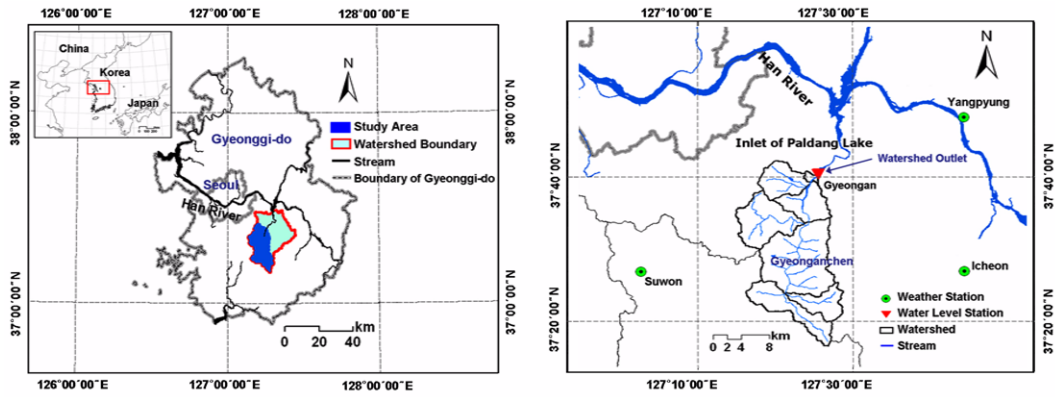Fig. 1. Vertical Water Balance of the SLURP Model (Kite, 2002)

Fig. 2. The Study Area

gauge station at the watershed outlet is located in the north-western part of South Korea within the latitude-longitude range of 37°0100E-37°0500E and 127°0100N-127°0300N (Fig. 2). The watershed stream is one of the main tributaries of Han River basin directly linked to the Paldang lake. The watershed has been continuously urbanized during the past couple of decades. The forest covers 60% and rice paddy and upland field occupy 10% and 13% respectively. The remaining land use types (urban, grassland, and bare ground) make up 5 to 7%. Predominantly, the grassland (golf course) increased from 2.0 km^2 in 1987 to 8.4 km^2 in 2004. The soil covers sand (8%), sandy loam (40%), clay loam (45%), and silty clay loam (8%) respectively. For the 30 years weather data from 1977 to 2006, the average annual temperature is 10.9 and the average annual precipitation is 1371.1 mm.

3.2 Map Data, Weather and Streamflow Data

The SLURP model requires elevation, soil, land use, Leaf Area Index (LAI) and weather data for assessment of water yield at the desired locations of watershed. Elevation data was rasterized from 1:5,000 vector map supplied by the Korea National Geography Institute (Fig. 3(a)). The water soil data was rasterized to a 30 m grid size from 1:25,000 vector map supplied by the Korea Rural Development Administration. Soil series and type are shown in Fig. 3(c) and Fig. 3(d) respectively.

For the future land use prediction, the five land use data were prepared using Landsat satellite images on 18th April 1987, 19th May 1991, 10th April 1996, 3rd June 2004 (TM) and 3rd June 2001 (ETM+) supplied by Remote Sensing Technology of Japan (RESTEC). The overall accuracy through maximum likelihood classification was 92.1%, 97.5%, 93.4%, 95.7% and 98.0% respectively.

For the future vegetation canopy prediction, the eight years (1997-2004) of monthly NDVI (Normalized Difference Vegetation Index) data were prepared from NOAA/AVHRR satellite images from March to November supplied by Korea Meteorological Administration.

For the model setup, the four years (1999-2002) daily weather data from three weather stations (Suwon, Icheon, and Yangpyeong) and streamflow data at the watershed outlet (Gyeongan water level gauging station) provided by the Ministry of Land, Transport and Maritime Affairs were prepared. The watershed was subdivided into 7 subbasins (Fig. 3(b)). The weather data regarding mean, maximum, minimum temperature (ºC), precipitation (mm), relative humidity (%), wind speed (m/sec), and sunshine hour (hr) were prepared for each subbasin of the watershed.

3.3 Model Calibration and Validation

The SLURP model was calibrated and validated using 2 years (1999-2000) and another 2 years (2001-2002) streamflow data
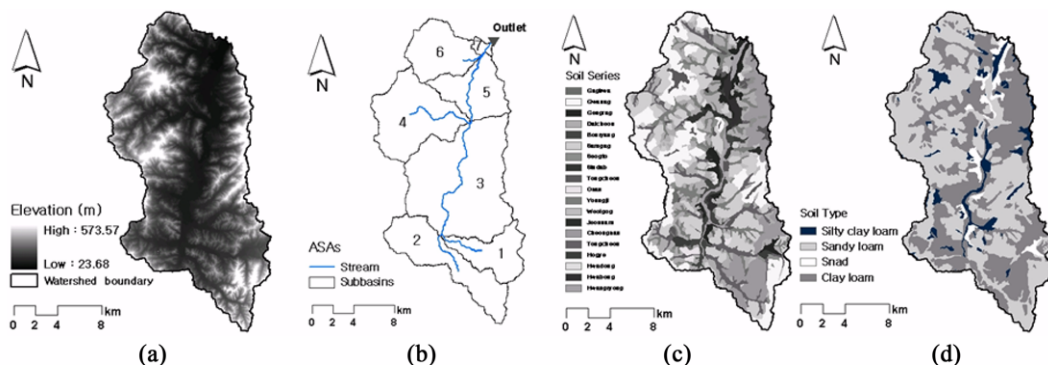

Fig. 3. GIS Data: (a) Elevation, (b) Subbasins, (c) Soil Series, (d) Soil Type

Table 1. The Calibrated Parameters of SLURP Model

Parameter	Sensitivity	Value		
		Forest	Paddy	Upland
Canopy capacity (mm)	Low	5	3	3
Albedo[1]	Medium	0.11	0.14	0.12
Canopy resist (s/m) [2]	Medium	48.1	26.7	38.1
Max. Crop height (m) [3]	Low	15	0.9	2
Crop start and end date [3]	Low	-	1 June - 10 September	-
Initial constants of snow store (mm)	Medium	32.0	20.0	20.0
Initial constants of slow store (%)	Medium	35.3	55.8	6.25
Maximum infiltration rate (mm/day)	High	32.8	15.5	36.26
Manning roughness, n	Low	0.05	0.01	0.08
Retention constant for fast store	Medium	10.5	6.3	7.95
Maximum capacity for fast store (mm)	High	230.8	100.5	141.2
Retention constant for slow store	High	55725.0	58935.0	84035.0
Maximum capacity for slow store (mm)	Medium	21400.0	30660.0	48670.0
Precipitation factor	High	1.0	1.0	1.0
Rain/snow division temperature (°C)	Low	0.0	0.0	0.0

[1] Zhou *et al.* (2003)
[2] National Institute Crop Science
[3] Korean Forest Research Institute

respectively. Through the sensitivity analysis and by using SCE-UA optimization technique (Duan *et al.*, 1994), the model parameters were calibrated. The objective functions for optimization are Nash-Sutcliffe Model Efficiency (ME) (Nash and Sutcliffe, 1970) and coefficient of determination (R^2).

The SLURP model requires parameter values for each land cover type listed in Table 1. The model was calibrated by differentiating two types of parameters (Linden and Woo, 2003). The first parameter values are soil physical parameters for soil moisture and subsurface flow listed in Table 2. In this study, the values of field capacity, wilting point and effective porosity were

adopted by Rawls *et al.* (1982). The second parameters were obtained by calibration, which affect the magnitude and timing of streamflow. Six parameters [viz. initial constants of slow store (groundwater storage), maximum infiltration rate, retention constant and maximum capacity for fast store (soil moisture storage), retention constant and maximum capacity for slow store] had high to medium sensitivities. The ET was especially sensitive to the initial constants of slow store.

The model was validated using the average value of calibrated parameters. Fig. 4 shows the comparison results of observed versus simulated streamflow. A statistical summary of model

Table 2. Soil Parameters of Three Major Land Use Classes

Lane use	Soil parameter		Percent covered for soil type			
			Sand	Sandy loam	Clay loam	Silty clay loam
Forest	F_c	0.24	5.7	58.3	35.7	0.3
	W_p	0.13				
	PO_e	0.38				
Rice paddy	F_c	0.27	7.1	34.5	46.4	11.9
	W_p	0.15				
	PO_e	0.37				
Upland field	F_c	0.26	7.9	36.0	47.7	8.3
	W_p	0.15				
	PO_e	0.37				

F_c: Field capacity (cm³/cm³), W_p: Wilting point (cm³/cm³), PO_e: Effective porosity (cm³/cm³)

Table 3. Summary of Model Calibration and Validation

Period		P (mm)	Observed		Simulated			RMSE (mm/day)	R^2	ME
			Q (mm)	QR (%)	Q (mm)	QR (%)	ET (mm)			
Calibration	1999	1340.6	752.8	56	697.3	52	413.9	3.5	0.79	0.77
	2000	1198.8	615.2	51	620.0	52	390.9	3.0	0.76	0.68
Verification	2001	982.0	492.2	50	511.3	52	413.6	3.2	0.71	0.69
	2002	1414.4	813.5	58	820.1	58	498.7	11.6	0.60	0.60
Average		1234.0	668.4	54	662.2	54	429.3	5.3	0.72	0.69

P: Precipitation, Q: Streamflow, QR: Runoff ratio, ET: Actual evapotranspiration
RMSE: Root mean square error, R^2: Coefficient of determination, ME: Nash-Sutcliffe model efficiency

calibration and validation is given in Table 3, and the results showed that the model was able to simulate the daily streamflow well with the R^2 and ME ranging from 0.60 to 0.79 and 0.60 to 0.77 respectively.

4. Data Preparation for Future Climate Change Impact Assessment

4.1 Future Climate Data from GCMs and Their Downscaling

The three GCM (MIROC3.2 hires, ECHAM-5OM, and HadCM3) data by three Special Report on Emissions Scenarios (SRES) climate change scenarios (A2, A1B, and B1) of the Intergovernmental Panel on Climate Change (IPCC) AR4 were adopted. Table 4 shows the characteristics of the GCMs. Here

A2 is "high" GHG emission scenario, A1B is "middle" GHG emission scenario, and B1 is "low" GHG emission scenario respectively. These experiments are started from the 20C3M (20th Century Climate Coupled Model) simulations and are run up to the year 2100. The data were obtained from the IPCC Data Distribution Center (www.mad.zmaw.de/IPCC_DDC/html/SRES_AR4/index.html). The spatial resolution of GCMs is too coarse to assess the regional effects of climate change (Snell *et al.*, 2000). As GCMs are inherently unable to represent local subgrid-scale features and dynamics, downscaling the GCM output to finer resolution is necessary (Zhang, 2007b).

In this study, a downscaling was performed by two steps. Firstly, the GCMs data was corrected to ensure that 30 years observed data (1977-2006, baseline period) and secondly, GCMs output of the same period have similar statistical properties using
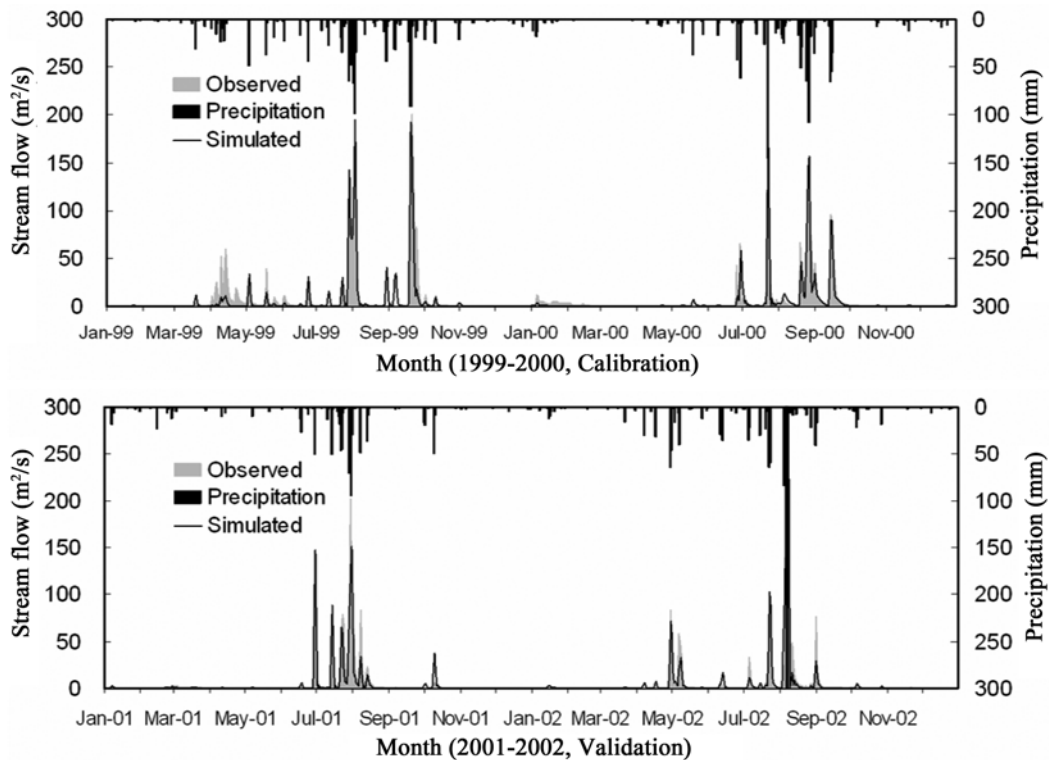

Fig. 4. The Calibration and Verification Results for Stream Flow (1999-2002)

Table 4. The GCM Data Adopted in this Study

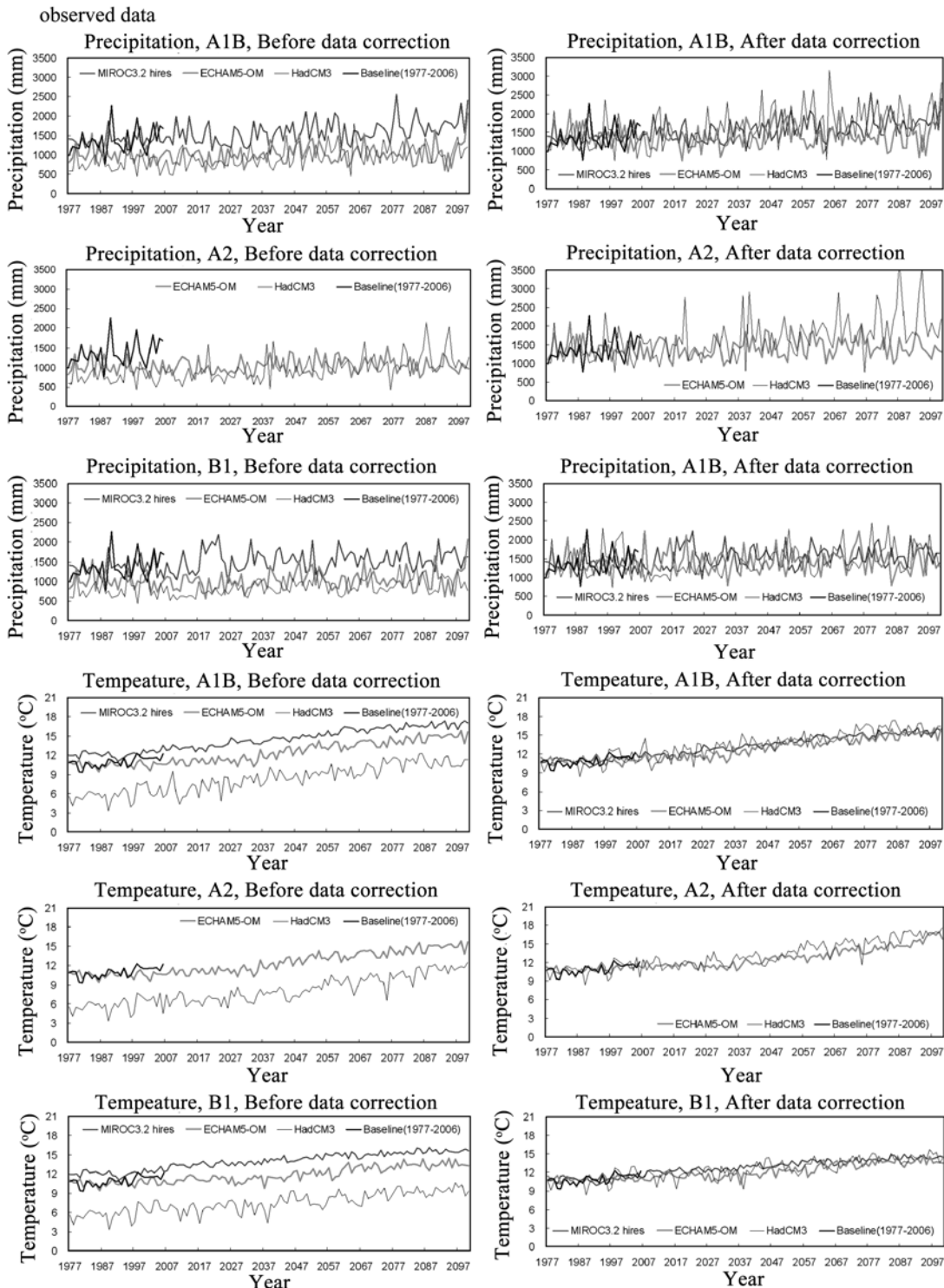|	Model	Center	Country	Scenario	Grid size
AR4 (2007)	MIROC3.2 hires	NIES	Japan	A1B, B1	320×160 ($1.1^\circ \times 1.1^\circ$)
	ECHAM5-OM	MPI-M	Germany	A2, A1B, B1	192×96 ($1.9^\circ \times 1.9^\circ$)
	HadCM3	UKMO	UK	A2, A1B, B1	96×73 ($3.7^\circ \times 2.5^\circ$)

Fig. 5. Adjusted Temperature and Precipitation Data for Three GCMs Data Using 30 Years (1977-2006) Historical Observed Data

the method by Alcamo *et al.* (1997) and Droogers and Aerts (2005) among the various statistical transformations. This method is generally accepted within the global change research community (IPCC-TGCIA, 1999). For temperature, the absolute changes between historical and future GCM time slices are added to measured values.

$$T'_{GCM,fut} = T_{meas} + (\overline{T}_{GCM,fut} - \overline{T}_{GCM,his}) \tag{1}$$

where, $T'_{GCM,fut}$ is the transformed future temperature, T_{meas} is the measured temperature for the 30 years baseline period, $\overline{T}_{GCM,fut}$ is the average future GCM temperature and $\overline{T}_{GCM,his}$ is the average historical GCM temperature. For precipitation, the relative changes between historical data and GCM output are applied to measured historical values.

$$P'_{GCM,fut} = P_{meas} \times (\overline{P}_{GCM,fut} / \overline{P}_{GCM,his}) \tag{2}$$

where, $P'_{GCM,fut}$ is the transformed future precipitation, P_{meas} is the measured precipitation, $\overline{P}_{GCM,fut}$ is the average future GCM precipitation and $\overline{P}_{GCM,his}$ is the average historical GCM precipitation. Fig. 5 shows the future adjusted temperature and precipitation using the 30 years observed data.

Secondly, the GCM data were downscaled using Change Factor (CF) method (Diaz-nieto and Wilby, 2005; Wilby and Harris, 2006). Monthly mean changes in equivalent variables from the 30 years observed data and three GCM data for three future time periods: 2020s (2010-2039), 2050s (2040-2069) and 2080s (2070-2099) were calculated for the GCM grid cell. The percent changes in monthly mean were applied to each day of 2002 weather data (selected as a base year for future assessment) of each weather station. The procedure was applied for each weather data. The CF method assumes that the spatial pattern of the present climate remains unchanged in the future. However, the key advantage of CF approach is the direct scaling of the scenario in line with changes suggested by the GCM (Diaz-nieto and Wilby, 2005).

Fig. 6 shows the changes in monthly temperature and precipitation by CF downscaling. Among the three GCMs, the biggest change of temperature was + 7.3°C in summer season of 2080 HadCM3 A2 scenario. The biggest differences of other three seasons were + 5.1°C in spring for 2080 HadCM3 A2, and + 5.0°C and + 6.2°C in autumn and winter for 2080 MIROC3.2 hires A1B scenario. Meanwhile, the downward tendency of temperature was also appeared in winter season of HadCM3. For the 2020 and 2050 winter seasons, the biggest decreases were 4.4
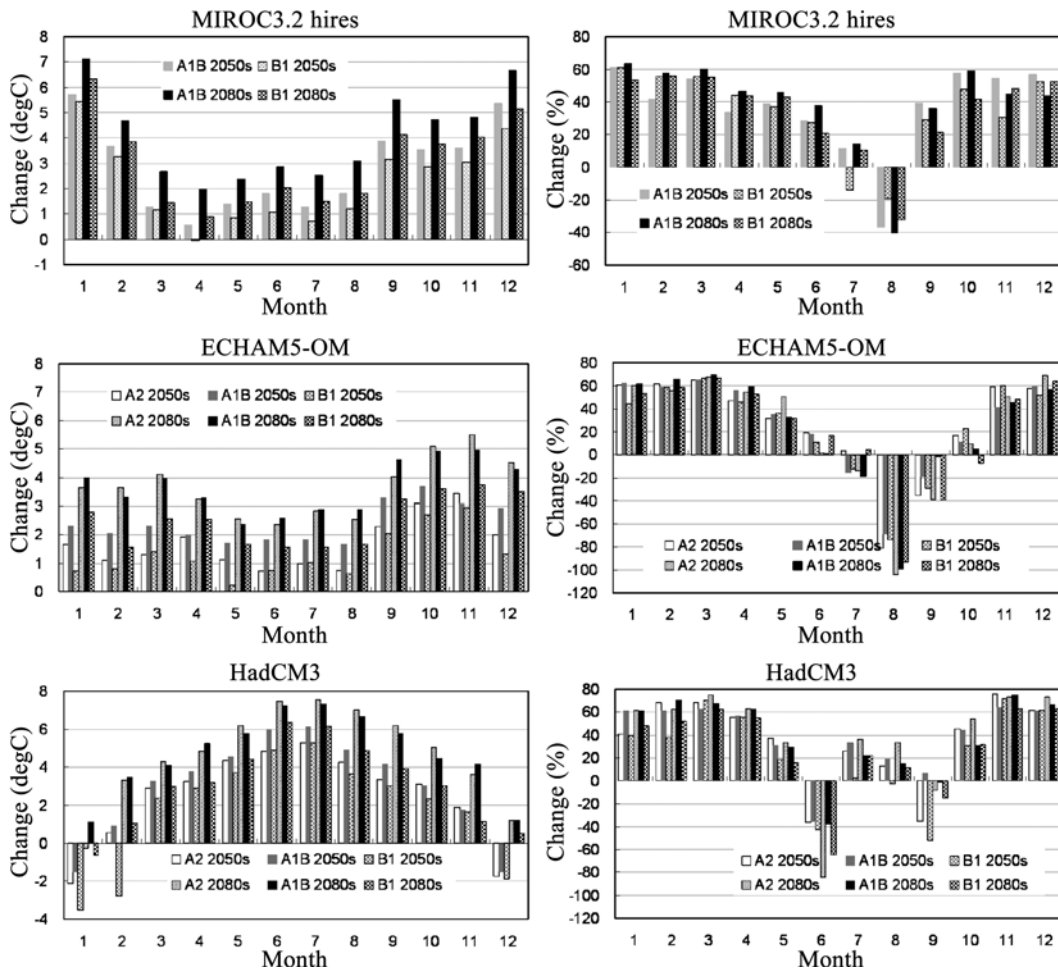

Fig. 6. Changes in Temperature (Left) and Precipitation (Right) by CF Downscaling for Three GCMs

Table 5. The Landsat Land Use from 1987 to 2004 and the CA-Markov Predicted Land Use of 2004, 2020, 2050 and 2080

Year		Land use class							
		Water	Forest	Urban	Grassland	Bare ground	Rice paddy	Upland field	Total
Landsat (%)	1987	0.3	58.5	4.4	2.0	4.5	17.3	12.9	100.0
	1991	0.3	60.2	4.1	3.7	10.5	15.5	5.6	100.0
	1996	0.4	57.3	4.3	2.8	6.6	16.3	12.2	100.0
	2001	0.2	60.1	5.0	5.1	6.4	10.4	12.8	100.0
	2004	0.3	54.4	5.7	8.4	8.6	9.7	12.9	100.0
CA-Markov (%)	2004	0.5	56.1	14.2	8.9	4.8	8.2	8.1	100.0
	2020	0.6	52.2	18.2	9.6	8.0	6.2	6.2	100.0
	2050	0.6	50.8	19.5	10.9	7.5	5.8	5.8	100.0
	2080	0.6	49.3	19.2	12.2	8.1	6.3	6.3	100.0

ºC and 2.7ºC for HadCM3 B1 scenario respectively. The future precipitation showed general tendency of decrease for summer season for all the three GCMs except 2050 and 2080 HadCM3 scenarios. Other three seasons showed the increase tendency on the whole. Among the three GCMs, the biggest change of precipitation was + 65.2% in winter season of 2080 HadCM3 A2 scenario. The biggest differences of other three seasons were + 59.4% in spring of 2080 HadCM3 A2, + 54.1% in autumn of MIROC3.2 hires, and + 65.2% in winter of 2080 HadCM3 A2 scenario.

The monthly variations are expected to detect the impact on future hydrologic cycle. The monthly temperature change of HadCM3 shows somewhat different change pattern comparing with two other GCMs. We can infer that the HadCM3 temperature will intensify the heat of summer and the coldness of winter season, while MIROC3.2 hires and ECHAM5-OM will give warming for the whole season. The monthly precipitation change of the three GCMs shows similar trends. The special different feature is that the big decrease in rainfall amount is found in August for MIROC3.2 hires and ECHAM5-OM and in June for HadCM3 respectively.

4.2 Future Land Use Change Prediction by the Modified CA-Markov Technique

The CA-Markov (Thomas, 2006) is a combined technique of Markov Chain (Turner, 1987) and Cellular Automata (CA) (Clarke at al., 1998). Markov Chain model handles lattice-based GIS data or satellite images, and reflects the changed tendency of present land use. The transition probability is fixed for a given time interval, but this makes difficult to trace the actual land cover change. If we consider the change over a fixed interval, the processing of spatial data that have sudden change is difficult. This difficulty can be supplemented using CA which is a nonlinear dynamic model that continuously applies distance directions and the changed state of regional contiguity to cells. The changed state of cell can be estimated, together with its complex characteristics and conformation, through recursive analysis. In the modified method (Lee and Kim, 2007), a

logarithmic function was reflected to consider the trend of past land use changes of each land use class using time series land use data. Data for water quality protection areas and greenbelt areas, which are restricted for land cover development by the government, were included to consider the social factor in the prediction. In addition, the minimal preserving probability, which was defined as the percentage for the upper limits of land cover change between land cover classes in the process of prediction, was applied to prevent unrealistic predictions of future land cover.

Using the 1987 and 1996 land use, 2004 CA-Markov land use was predicted and the result was compared with the 2004 Landsat land use. The modified CA-Markov technique was evaluated by three indices (α, β, and γ) to compare that the spatial fit between the observed and the predicted. The first index α is the ratio of matched cell number of the predicted to the total cell number of the observed, and ranges from 0 to 1. The second index β is the ratio of matched cell number of the predicted to the total cell number as sum of sets of the observed and the predicted, and ranges from 0 to 1. The third index γ is the ratio of cell number of the predicted to the cell number of the observed, and ranges from 0 to 2. For all indices, the prediction accuracy of spatial fit is perfect when the value of each index is 1.0. For α and β, the prediction accuracy decreases as the value approaches to 0. For γ, the prediction accuracy decreases as the value goes away from 1 to 0 or 2. As a result, the modified CA-Markov α, β and γ values were 0.70, 0.68, and 0.96 while the values of original CA-Markov were 0.62, 0.57, and 0.87 respectively.

The future predicted land uses of 2020s, 2050s and 2080s are summarized in Table 5. The results showed that the forest and rice paddy area decreased 10.8% and 6.2% respectively while the urban area increased 14.2%.

4.3 Future Vegetation Canopy using NOAA/AVHRR Satellite Image

To predict the future vegetation canopy condition, a linear regression between the monthly NDVI from NOAA/AVHRR satellite image and the monthly mean air temperature was

Table 6. The Future Predicted Monthly NDVIs for Three GCMs

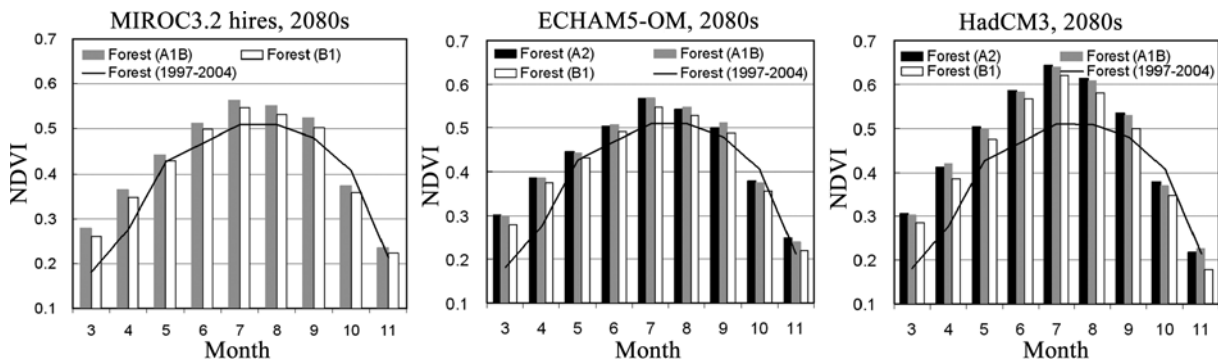| Period		Baseline	MIROC3.2 hires		ECHAM5-OM			HadCM3		
			A1B	B1	A2	A1B	B1	A2	A1B	B1
1997-2006	Max.	0.51	-	-	-	-	-	-	-	-
	Min.	0.15	-	-	-	-	-	-	-	-
2020s	Max.	-	0.52	0.52	0.52	0.52	0.53	0.58	0.60	0.58
	Min.	-	0.15	0.15	0.13	0.14	0.13	0.12	0.12	0.12
2050s	Max.	-	0.54	0.53	0.54	0.55	0.54	0.61	0.59	0.31
	Min.	-	0.17	0.16	0.16	0.16	0.16	0.14	0.14	0.14
2080s	Max.	-	0.56	0.55	0.57	0.57	0.55	0.64	0.64	0.62
	Min.	-	0.18	0.17	0.19	0.19	0.17	0.17	0.18	0.13

Fig. 7. The Future 2080s Predicted Monthly Forest NDVIs for A1B, A2 and B1 Scenarios

accomplished for each land cover. The monthly NDVIs of each land use from December to February could not be prepared because of snow cover, thus they were extrapolated from the regression equation.

Table 6 shows the 2020s, 2050s, and 2080s predicted maximum and minimum value of monthly NDVIs based on the future temperature scenarios. The highest NDVI values for three GCMs was 0.56 (MIROC 3.2 hires, A1B), 0.57 (ECHAM5-OM, A2 and A1B) and 0.64 (HadCM3, A2 and A1B) by the 2080s while the current highest NDVI value was 0.51. Fig. 7 shows the future monthly changes of NDVI for forest land use.

5. Evaluation of Future Climate Change Impact on Hydrologic Response

A key for long-term planning of water resources considering future change in the pattern of climate, water availability in a watershed is not only the possible change to annual hydrologic components but also how seasonal hydrologic components may change. For the evaluation of climate change impact on hydrological components such as streamflow, ET, soil moisture and groundwater recharge, the SLURP model was run using the future climate, land use, and vegetation canopy data with 2002 as a base year.

Table 7 summarizes the future predicted annual hydrologic components for A2, A1B and B1 scenarios of three GCMs, and

Fig. 8 shows the future predicted seasonal streamflow, ET and groundwater recharge. For the 2020s scenarios as in Table 7, the annual streamflow were predicted to change between - 14.5% by ECHAM5-OM under A1B and +25.8% by HadCM3 under A1B scenario. For the 2050s scenarios, the annual streamflow were predicted to change between -3.7% by ECHAM5-OM under B1 and +42.1% by HadCM3 under A1B scenario. For the 2080s scenarios, the annual streamflow were predicted to change between -1.3% by ECHAM5-OM under B1 and +52.8% by HadCM3 under A2 scenario. While keeping in mind the uncertainties associated with longer term predictions, MIROC3.2 hires and HadCM3 showed increase tendency in annual streamflow up to 21.4% for 2080 A1B and 52.8% for 2080 A2 scenario respectively, while ECHAM5-OM showed variations from -14.5% for 2020 A1B to +8.9% for 2050 A1B scenario. For the seasonal streamflow changes in Fig. 8, the spring streamflow of three GCMs showed clear increases while the summer streamflow showed overall decrease for MIROC3.2 hires and ECHAM5-OM and increase for HadCM3. This result is directly linked to the future monthly precipitation changes as shown in Fig. 6. The HadCM3 has rainfall decrease in June and increases in July and August while the other two GCMs have overall rainfall increase in June and decreases in July and August. Regardless of the scenarios, the great change in streamflow was appeared for the months of April and August.

ET is an important element for the hydrological cycle (Kite,

Table 7. Summary of the Future Predicted Annual Hydrologic Components for Three GCMs

Period	T (°C)	T difference (°C)	P (mm)	P variation (%)	Q (mm) [QR (%)]	Q variation (%)	ET (mm) [ETR (%)]	SM (%)	GW (mm)
[Baseline]									
2002	11.6	-	1414.4	-	820.1 [58]	-	498.7 [35]	17.0	319.4
MIROC3.2 hires [A1B]									
2020s	12.7	+1.1	1578.9	+10.4	916.2 [58]	+10.5	576.2 [36]	17.8	344.7
2050s	14.4	+2.8	1640.8	+13.8	946.8 [58]	+13.4	585.0 [36]	17.9	351.9
2080s	15.6	+4.0	1765.0	+19.9	1043.2 [59]	+21.4	659.4 [37]	17.9	358.6
MIROC3.2 hires [B1]									
2020s	12.8	+1.2	1621.6	+12.8	940.1 [58]	+12.8	585.8 [36]	17.9	355.3
2050s	13.8	+2.2	1691.3	+16.4	1013.1 [60]	+19.1	593.5 [35]	17.9	355.1
2080s	14.6	+3.0	1652.6	+14.4	958.6 [58]	+14.4	630.4 [38]	17.8	346.0
ECHAM5-OM [A2]									
2020s	11.9	+0.3	1438.7	+1.7	810.9 [56]	-1.1	687.6 [48]	17.1	277.5
2050s	13.3	+1.7	1487.0	+4.9	820.4 [55]	0.0	720.5 [48]	17.3	293.6
2080s	15.2	+3.6	1499.3	+5.7	827.4 [55]	+0.9	758.4 [51]	17.3	288.4
ECHAM5-OM [A1B]									
2020s	11.9	+0.3	1343.6	-5.3	716.3 [53]	-14.5	689.0 [51]	17.1	279.9
2050s	13.9	+2.3	1557.0	+9.2	900.2 [58]	+8.9	715.6 [46]	17.3	294.4
2080s	15.2	+3.6	1503.7	+2.9	847.7 [56]	+3.3	757.1 [50]	17.3	279.9
ECHAM5-OM [B1]									
2020s	11.8	+0.2	1440.2	+1.8	788.7 [55]	-4.0	702.6 [49]	17.3	288.6
2050s	12.9	+1.3	1439.2	+1.7	791.1 [55]	-3.7	680.8 [47]	17.4	285.7
2080s	14.1	+2.5	1471.5	+3.9	809.5 [55]	-1.3	722.7 [49]	17.4	285.4
HadCM3 [A2]									
2020s	12.4	+0.8	1667.6	+15.2	1018.2 [61]	+19.5	738.4 [44]	17.1	308.3
2050s	14.1	+2.5	2014.5	+29.8	1315.9 [65]	+37.7	821.9 [41]	17.4	344.9
2080s	16.3	+4.7	2461.6	+42.5	1737.7 [71]	+52.8	853.6 [35]	17.5	386.7
HadCM3 [A1B]									
2020s	12.8	+1.2	1764.4	+19.8	1105.1 [63]	+25.8	775.2 [44]	17.1	312.0
2050s	14.5	+2.9	2121.1	+33.3	1417.6 [67]	+42.1	803.9 [38]	17.5	364.2
2080s	16.3	+4.7	2095.6	+32.5	1390.8 [66]	+41.0	859.6 [41]	17.3	352.4
HadCM3 [B1]									
2020s	12.0	+0.4	1348.5	-4.9	722.5 [54]	-13.5	736.0 [55]	16.9	283.4
2050s	13.4	+1.8	1759.3	+19.6	1101.6 [63]	+25.6	795.4 [45]	17.0	308.1
2080s	14.6	+3.0	1902.8	+25.7	1237.1 [65]	+33.7	767.2 [40]	17.2	340.5

P: Precipitation, Q: Streamflow, QR: Runoff ratio, ET: Actual evapotranspiration
ETR: Actual evapotranspiration ratio, SM: Soil moisture, GW: Groundwater recharge

2000). In the watershed, 35% of the 2002 precipitation was returned to the atmosphere by evaporation and transpiration as in Table 7. The portion of predicted ET about future precipitation was 35%-38% in MIROC3.2 hires, 46%-51% in ECHAM5-OM, and 38%-55% in HadCM3 respectively. It is noticed that the future increase of ET was from the increase of temperature under the increased precipitation as seen in Table 7 (T difference and P variation). The future ET increased in all seasons, especially showing big increases in spring and summer for all GCMs. The future soil moisture content slightly increased compared to 2002 soil moisture. In spite of the big increase of future ET, the future maintenance of soil moisture even increase less than 1% can be explained by the overall increase of precipitation except summer season, which covers the new ET
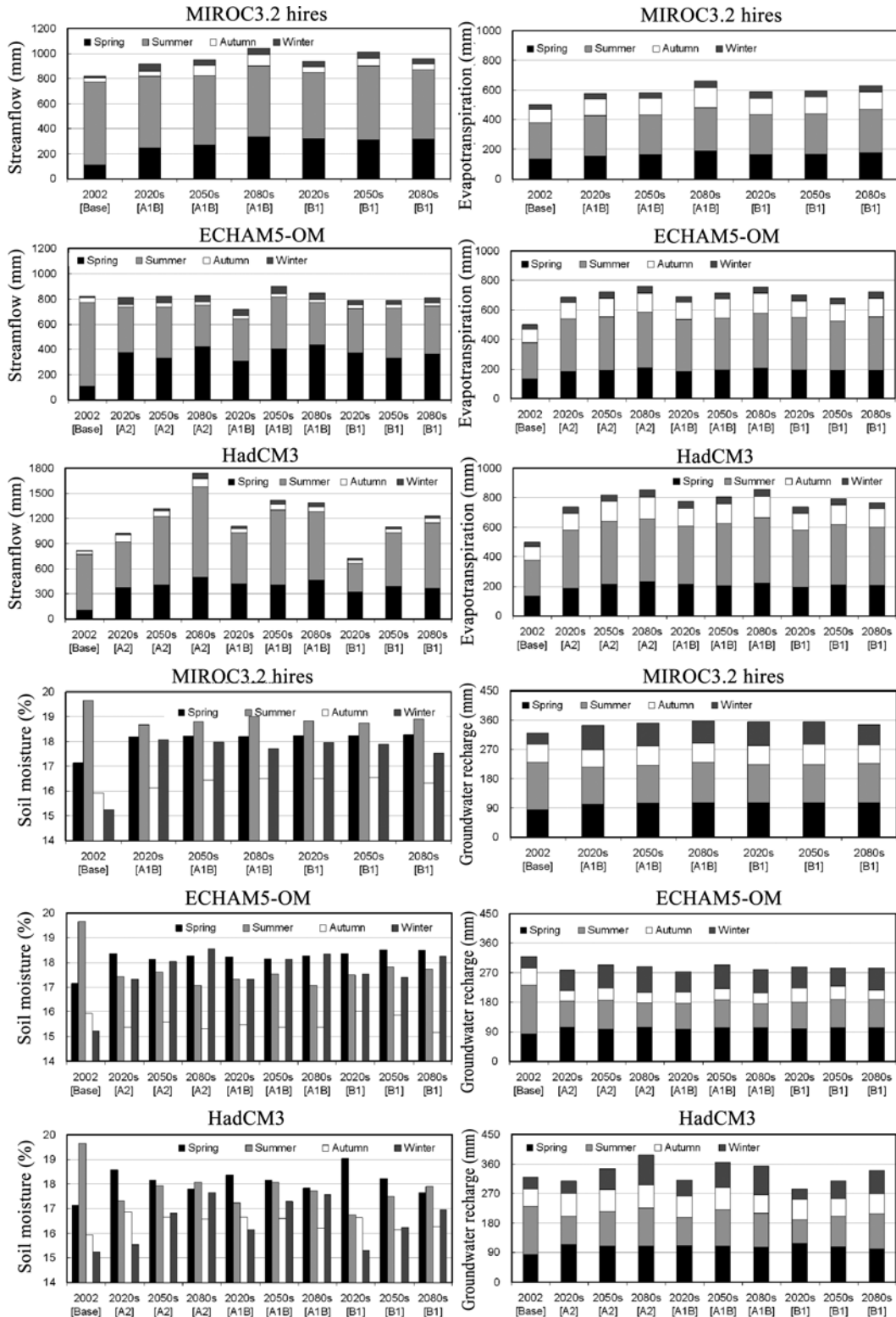
Fig. 8. The Future Seasonal Mean Hydrologic Components for A2, A1B and B1 Scenarios of Three GCMs

demand by the increased temperature. The increase of soil moisture resulted in the increase of groundwater recharge except ECHAM5-OM. It can be explained that the opposite result of ECHAM5-OM groundwater recharge came from the relatively small amount of future precipitation increase comparing with the other two GCMs precipitation.

Although the predicted hydrological scenarios have high uncertainty associated with future climates of GCMs, the consi-

derable streamflow change especially during the summer period in our country certainly gives an increasingly difficult task in managing future water resources throughout the year. The clear big increase of ET in the future can cause more frequent and severe droughts by the water deficit of the watershed especially if rainfalls are concentrated in a certain period.

6. Conclusions

The basin-level hydrological model SLURP was applied to assess the future potential impact of climate change on streamflow of a 260.4 km² watershed located in the northwestern part of South Korea. Before the future assessment, the SLURP model was calibrated and validated by comparing daily observed with simulated streamflow results for 4 years (1999-2002). The average Nash-Sutcliffe model efficiency of model validation was 0.69.

For the future climate data, the three GCMs (MIROC3.2 hires, ECHAM-5OM and HadCM3) data were downscaled by the Change Factor method after correcting the data using the 30 years observed data (1977-2006) to have similar statistical properties. The HadCM3 temperature intensified the heat of summer and the coldness of winter season, while MIROC3.2 hires and ECHAM5-OM give warming for the whole season. The future precipitation showed general tendency of decrease up to 64.3% (2020 HadCM3 B1) for summer season for all three GCMs scenario. Other three seasons showed the increase tendency up to 65.2% (2080 HadCM3 A2) on the whole. To reduce the uncertainty of future land surface conditions, the land use and vegetation canopy prediction were tried by CA-Markov technique and NOAA NDVI versus temperature relationship respectively. The 2080 land uses showed that the forest and paddy areas decreased 10.8% and 6.2% respectively while the urban area increased 14.2%. The future 2080 highest NDVI value was 0.64 while the current highest NDVI value was 0.53.

The future assessment showed that MIROC3.2 hires and HadCM3 showed increase tendency in annual streamflow up to 21.4% for 2080 A1B and 52.8% for 2080 A2 scenario respectively, while ECHAM5-OM showed variations from -14.5% for 2020 A1B to +8.9% for 2050 A1B. The seasonal streamflow showed that the spring streamflow of three GCMs clearly increased while the summer streamflow decreased for MIROC3.2 hires and ECHAM5-OM and increased for HadCM3. The portion of future predicted ET about precipitation increased up to 3% in MIROC3.2 hires, 16% in ECHAM5-OM, and 20% in HadCM3 respectively. The future ET increased in all seasons, especially showing big increases in spring and summer for all GCMs. The future soil moisture content slightly increased compared to 2002 soil moisture. The increase of soil moisture resulted in the increase of groundwater recharge except ECHAM5-OM. The future hydrologic conditions cannot be projected exactly due to the uncertainty in climate change scenarios and the statistically downscaled GCMs data as in this study. A stochastic daily time scale weather generation that considers wet

and dry spell lengths may produce more plausible scenarios for future flood and drought conditions. Even though the annual change and seasonal variation of hydrological components due to future temperature increase and precipitation change in possible ways should be evaluated in order to promote more sustainable water availability for a stream watershed of our country.

References

Ahn, J. H., Yoo, C. S., and Yoon, Y. N. (2001). "An analysis of hydrologic changes in Daechung dam basin using GCM simulation results due to global warming." *Journal of Korean Water Resources Association*, Vol. 34, No. 4, pp. 335-345.

Alcamo, J., Döll, P., Kaspar, F., and Siebert, S. (1997). *Global change and global scenarios of water use and availability: An application of Water GAP 1.0. Report A9701*, Center for Environmental Systems Research, University of Kassel, Germany.

Aleix S. C., Juan, B. V., Javier, G. P., Kate, B., Luis, J. M., and Thomas, M. (2007). "Modeling climate change impacts-and uncertainty-on the hydrology of a riparian system." *Journal of Hydrology*, Vol. 347, Nos. 1-2, pp. 48-66.

Andersen, J., Dybkjaer, G., Jensen, K. H., Refsgaard, J. C., and Rasmussen, K. (2002). "Use of remotely sensed precipitation and leaf area index in a distributed hydrological model." *Journal of Hydrology*, Vol. 264, Nos. 1-4, pp. 34-50.

Andersson, L., Wilk, J., Todd, M. C., Hughes, D. A., Earle, A., Kniveton, D., Layberry, R., and Savenije, H. G. (2006). "Impact of climate change and development scenarios on flow patterns in the Okavango River." *Journal of Hydrology*, Vol. 331, Nos. 1-2, pp. 43-57.

Arnell, N. W. (1999). "Climate change and global water resources." *Global Environmental Change*, Vol. 9, No. 1, pp. S31-S49.

Clarke, K. C. and Gaydos, L. J. (1998). "Loose-coupling a cellular automata model and GIS: Long-term urban growth prediction for San Francisco and Washington/Baltimore." *Journal of Geographical Information Science*, Vol. 12, No. 7, pp. 699-714.

Diaz-nieto, J. and Wilby, R. L. (2005). "A comparison of statistical downscaling and climate change factor methods: Impacts on low flows in the River Thames." *Climatic Change*, Vol. 69, Nos. 2-3, pp. 245-268.

Doogers, P. and Aerts, J. (2005). "Adaptation strategies to climate change and climate variability: A comparative study between seven contrasting river basins." *Physics and Chemistry of the Earth*, Vol. 30, No. 6, pp. 339-346.

Duan, Q., Sorooshian, S. S., and Gupta, V. K. (1994). "Optimal use of the SCE-UA global optimization method for calibrating watershed models." *Journal of Hydrology*, Vol. 158, Nos. 3-4, pp. 265-284.

Forch, G., Garde, F., and Jensen, J. (1996). "Climate change and design criteria in water resources management: A regional case study." *Atmospheric Research*, Vol. 42, No. 1, pp. 33-51.

Gellens, D. and Rouline, E. (1998). "Streamflow responses of Belgian catchments to IPCC climate change scenarios." *Journal of Hydrology*, Vol. 210, Nos. 1-4, pp. 242-258.

Ghosh, S. and Mujumdar, P. P. (2008)." Statistical downscaling of GCM simulations to streamflow using relevance vector machine." *Advances in Water Resources*, Vol. 31, No. 1, pp. 132-146.

IPCC (2001). *Climate change 2001: Scientific basis*, In: Contribution of Working Group III to the Third Assessment Report of the Intergovernmental Panel on Climate Change, Metz, B. *et al.* (ed.), Published for the Intergovernmental Panel on Climate Change [by] Cambridge University Press, Cambridge, UK, New York, USA.

IPCC Data Distribution Centre, Available at:www.mad.zmaw.de/IPCC_DDC/html/SRES_AR4/index.html.

IPCC-TGCIA (1999). *Guidelines on the use of scenario data for climate impact and adaptation assessment*, Version 1, In: Carter, T. R., Hulme, M., Lal, M. (eds.), Intergovernmental Panel on Climate Change Task Group on Scenarios for Climate Impact Assessment, p. 69.

Kite, G. W. (1975). "Performance of two deterministic hydrological models." *IASH-AISH Publication*, Vol. 115, pp. 136-142.

Kite, G. W. (1993). "Application of a land class hydrological model to climatic change." *Water Resources Research*, Vol. 29, No. 7, pp. 2377-2384.

Kite, G. W. (2000). "Using a basin-scale hydrological model to estimate crop transpiration and soil evaporation." *Journal of Hydrology*, Vol. 229, Nos. 1-2, pp. 59-69.

Kite, G. W. (2002). *Manual for the SLURP hydrological model*, V. 12.2.

Kite, G. W., Dalton, A., and Dion, K. (1994). "Simulation of streamflow in a macro-scale watershed using GCM data." *Water Resources Research,* Vol. 30, No. 5, pp. 1546-1559.

Lee, Y. J. and Kim, S. J. (2007). "A modified CA-Markov technique for prediction of future land use change." *Journal of the Korean Society of Civil Engineers*, Vol. 57, No. 6D, pp. 809-817.

Legates, D. R. and McCabe, G. J. (1999). "Evaluating the use of 'goodness of fit' measures in hydrologic and hydroclimatic model validation." *Water Resources Research*, Vol. 35, No. 1, pp. 233-241.

Linden, S. and Woo, M. K. (2003). "Transferability of hydrological model parameters between basins in data-sparse areas, subarctic Canada." *Journal of Hydrology*, Vol. 170, Nos. 3-4, pp. 182-194.

Merritt, W. S., Alila, Y., Barton, M., Taylor, B., Cohen, S., and Neilsen, D. (2006). "Hydrologic response to scenario of climate change in sub watersheds of the Okanagan basin, British Columbia." *Journal of Hydrology*, Vol. 326, Nos. 1-4, pp. 79-108.

Myneni, R. B. and Williams, D. L. (1994). "On the relationship between FPAR and NDVI." *Remote Sensing of Environment*, Vol. 49, pp. 200-211.

Nash, J. E. and Sutcliffe, J. V. (1970). "River flow forecasting through conceptual models: Part 1 - A discussion of principles." *Journal of Hydrology*, Vol. 10, No. 3, pp. 282-290.

Pruski, F. F. and Nearing, M. A. (2002). "Runoff and soil loss responses to changes in precipitation: A computer simulation study." *Journal of Soil and Water Conservation*, Vol. 57, No. 1, pp. 7-16.

Rawls, W. J., Brakensiek, D. L., and Saxton, K. E. (1982). "Estimation of soil water properties." *Transactions of the American Society of Agriculture Engineers*, Vol. 25, No. 5, pp. 1316-1320.

Sellers, P. J., Tucker, P. J., Collatz, G. J., Los, S. O., Justice, C. O., Dazlich, D. A., and Randall, D. A. (1994). "A global 1 degree by 1 degree NDVI data set for climate studies. Part 2: the generation of global fields of terrestrial biophysical parameters from NDVI." *Journal of Remote Sensing*, Vol. 15, No. 17, pp. 3519-3545.

Snell, S. E., Gopal, S., and Kaufmann, R. K. (2000). "Spatial interpolation of surface air temperatures using artificial neural networks: Evaluating their use for downscaling GCMs." *Journal of Climate*, Vol. 13, No. 5, pp. 886-895.

Thomas, H. and Laurence, H. M. (2006). "Modelling and projecting landuse and landcover changes with a cellular automaton in considering landscape trajectories: An improvement for simulation of plausible future states." *Journal of the European Association of Remote Sensing Laboratories*, Vol. 5, pp. 63-76.

Turner, M. G. (1987). "Spatial simulation of landscape changes in Georgia: A comparison of three transition models." *Landscape Ecology*, Vol. 1, No. 1, pp. 29-36.

Westmacott, J. R. and Burn, D. H. (1997). "Climate change effects on the hydrologic regime within the Churchill-Nelson river basin." *Journal of Hydrology*, Vol. 202, Nos. 1-4, pp. 263-279.

Wilby, R. L. and Harris, I. (2006). "A framework for assessing uncertainties in climate change impacts: Low-flow scenarios for the River Thames, UK." *Water Resources Research*, Vol. 42, No. W02419, pp. 1-10.

Zhang, G. H., Fu, S. H., Fang, W. H., Imura, H., and Zhang, X. C. (2007a). "Predicting effects of climate change on runoff in the Yellow River Basin of China." *American Society of Agricultural and Biological Engineers*, Vol. 50, No. 3, pp. 911-918.

Zhang, X., Srinivasan, R., and Hao, F. (2007b). "Predicting hydrologic response to climate change in the Luohe River Basin using the SWAT model." *American Society of Agricultural and Biological Engineers*, Vol. 50, No. 3, pp. 901-910.

Zhou, L., Dickinson, R. E., Tian, Y., Zeng, X., Dai, Y., Yang, Z. L., Schaaf, C. B., Gao, F., Jin, Y., Strahler, A., Myneni, R. B., Yu, H., and Shaikh, M. (2003). "Comparison of seasonal and spatial variations of albedos from Moderate-Resolution Imaging Spectroradiometer (MODIS) and Common Land Model." *Journal of Geophysical Research*, Vol. 108, No. 15, pp. 1-20.